Iraqi Journal of Natural Sciences and Nanotechnology IJNSN
Journal Homepage : https://publications.srp-center.iq/index.php/ijn

Long-Range Hybrid Plasmonic Waveguide of Graded-Index InGaAsP Active Layer Based on InP

Watheq Fahem Shneen[1,2*], Sabah Mahdi Mohammad Ameen[1]

[1]Department of Physics, College of Science, University of Basrah, Basrah, Iraq
[2]College of Science, University of Kufa, Iraq/An-Najaf

*Corresponding author: wathaqf.gnaby@uokufa.edu.iq

Keywords:
Hybrid plasmonic waveguide,
Graded index,
Propagation length,
Mode effective area,
Figure of merit.

Abstract

A hybrid plasmonic waveguide based on indium phosphide (InP) was proposed for nanoscale optical confinement and long-range propagation at a wavelength of 1.55 µm. The waveguide consists of an InGaAsP layer designed as a ridge with a gold cap. The InGaAsP materials are suitable for InP substrates. The refractive index of $In_{1-x}Ga_xAs_yP_{1-y}$ was graded by changing the mole fraction to improve the confinement and propagation length compared with the conventional one. Changing only the y parameter with constant x results in a propagation length increase compared to the inverse case, changing only the parameter x. This parallels good results in the mode effective area (A_{eff}) and figure-of-merit (FoM) for the exact condition of changing y, expressing a good confinement condition. A propagation length of 40 µm is achieved with better confinement than the standard hybrid case. The designs proposed in this paper were simulated using COMSOL Multiphysics.

Introduction

The SPP is the coupling of a photon with free electrons at the interface between the metal and an insulator. Plasmonic waveguides may manipulate optical fields at the nanoscale by converting light to surface plasmon polaritons (SPPs). The hybrid surface plasmonic polariton (HSPP) waveguide in most structures of optical integrated circuits has two basic parameters that should be studied, that is, the propagation length Lp and confinement factor. By increasing Lp in parallel with a good quantitative confinement pattern, the waveguide

 DOI: https://doi.org/10.47758/ijnsn.v5i1.120

will operate effectively. However, there is an inverse relationship between these two properties. By manufacturing processes and offering certain models, we can overcome this barrier and raise one while preserving the other without sacrificing efficiency. There are many proposals and solutions, including changes in materials and shape. In one of the layers that make up the structure ($In_{1-x}Ga_xAs_yP_{1-y}$ semiconductor)[1] [1] [2], which is a quaternary material, we can determine the specifications and properties of this material from Ref. [3] and [4], where doping will be applied to produce a graded refractive index. This design could serve as a potential option for many nanophotonic components, optoelectronic integrated circuit structures [5] [6] [7] [8], and complementary metal oxide semiconductors (CMOS)[7] [9] [10]. Additionally, $In_xGa_{1-x}As$, which is a ternary compound, can be used, and its properties are viewed in Refs. [11] and [12].

In the graded refractive index, the light ray experiences refraction gradually and thus bends toward the center, which represents the interface between the metal and the insulator, allowing propagation of the ray in a curved path. This means that the light upon traveling is continuously refracted and bends. Therefore, the light rays do not propagate by following a straight line; rather, they follow a parabolic path due to nonuniformity in the refractive index of the medium.

We have a structure consisting of a ridge waveguide of a noble metal (gold) that is above a layer of InP[1], and between the InP layer and substrate (which is of the same substance InP), there is an intermediate layer of quaternary semiconductor (InGaAsP)[13][14][1]. InGaAsP lattices are suitable for that of an InP substrate[15] [16] in the wavelength between 1.3-1.7 μm region, a spectral area in which low-loss, low-dispersion optical fibers are available[17][18]. This layer focuses on employing the graded index, which is x and y (mole fractions) in the instance of the semiconductor ($In_{1-x}Ga_xAs_yP_{1-y}$) quaternary, to offer a variable refractive index as a graded refractive index[19]. To reach the best structures, we will work here on the following cases: the first is taking a constant mole fraction y with changing x, and the second is changing x for material $In_xGa_{1-x}As$[12][20]. The two cases are compared with the results of the conventional case that we took from the published works in the literature without a graded procedure.

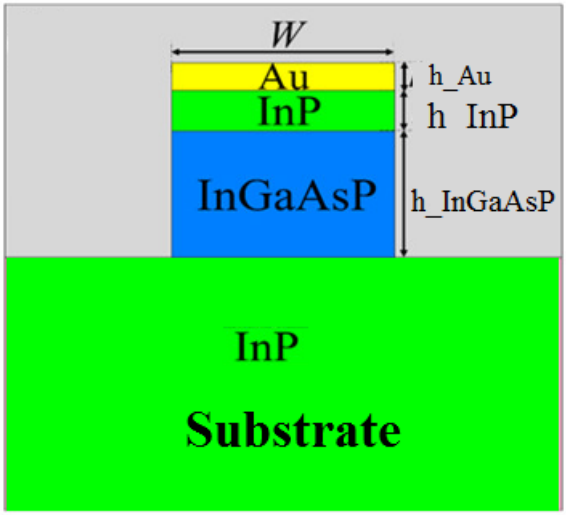

Figure 1 Structure of HSPP.

The InP-based orthodox waveguide contains an InGaAsP core layer with a thickness of 500 nm and an InP upper cladding layer with a thickness of 160 nm on a semi-insulating InP substrate. Gold (Au) with a thickness of 110 nm caps the layer stack of the hybrid plasmonic waveguide.

Simulation graded index

There is a relation between the mole fractions x and y in quaternary compounds, such as the structure used here, for a wavelength of 1.55 μm:

$$x = \frac{0.1896y}{0.4176 - 0.0125y} \qquad (1)$$

The relationship between the real (n_r) and imaginary (n_i) refractive indices with composition fractions for a wavelength of 1.55 μm is as follows[21] [22] [23] [24]

$$\left.\begin{aligned} n_r &= (12.35 + 1.62y - 0.055y^2)^{0.5} \\ n_i &= \frac{\lambda\alpha}{4\pi} \end{aligned}\right] \qquad (2)$$

where α is the optical absorption of InGaAsP. The refractive index according to the x mole fraction for ternary compound $In_xGa_{1-x}As$ is known from Ref. [20].

The structure generated by using COMSOL software simulates steps to calculate the guided eigenmodes of the hybrid plasmonic waveguide used in this work. This explains the four major steps to performing mode-solving simulations. The first step is to define the geometrical parameters of the waveguide and the refractive indices of the materials, as shown in Table 1, such as the piecewise and analytic functions in Fig. 2 and Fig. 3, respectively,

as well as set the graded refractive index equation using Eq. 3 and graded profile Eq. 4. Using experimentation, since this equation is a mathematical relationship, the realist representation is several layers of the same material, but with different doping, creating a graded refractive index. Designing the geometry, applying the boundary conditions, and defining the mesh (Fig. 4) is the second step. Then, the eigenmode solver based on the finite element method is chosen to calculate the hybrid modes of the waveguide. Finally, the results, such as the electric field norm distribution for mode TM, can be visualized in a 2D surface plot, which results from a vertical cross-sectional slice in the waveguide, or by the applied 1D plot.

$$n_g = \mathrm{n_{min}} * \sqrt{1 + 2\,\Delta\, \mathrm{e}^{-2\mathrm{y}/\mathrm{h_{core}}}} \qquad (3)$$

where

$$\Delta = \frac{\mathrm{n}_p^2 - \mathrm{n}_{min}^2}{2\mathrm{n}_{min}^2} \qquad (4)$$

where n_p , n_{min} are the peak and minimum values of the refractive index for the graded material. When we use electromagnetic waves, frequency domain (emw), the major selling point node for this physics interface is the wave equation, Electric[25]. The governing equation is as follows:

$$\left.\begin{array}{c} \nabla \times \mu_r^{-1}(\nabla \times \mathbf{E}) - k_0^2\left(\epsilon_r - \dfrac{j\sigma}{\omega\epsilon_0}\right)\mathbf{E} = \mathbf{0} \\ \alpha = j\beta + \delta_z = -\lambda \\ \mathbf{E}(x,y,z) = \grave{\mathbf{E}}(x,y)e^{-\alpha z} \end{array}\right\} \qquad (5)$$

As well as the boundary condition Perfect Electric Conductor (**n** × **E=0**) and appropriate mesh in Fig. 4, we obtain the following results. Show us the Norm E, Poynting vector **p**(x,y), and energy density W findings.

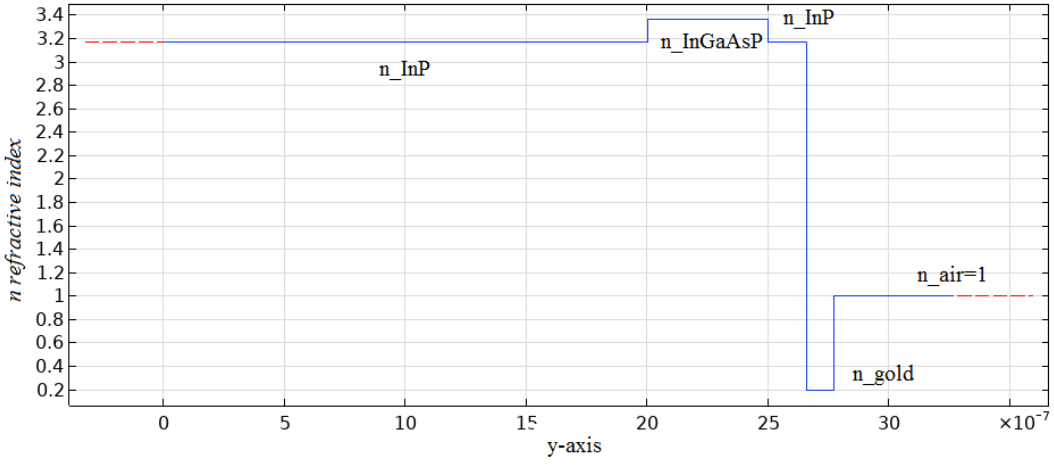

©SRP 2024, DOI: https://doi.org/10.47758/ijnsn.v5i1.120

Figure 2 Refractive index for all layers used in the structure

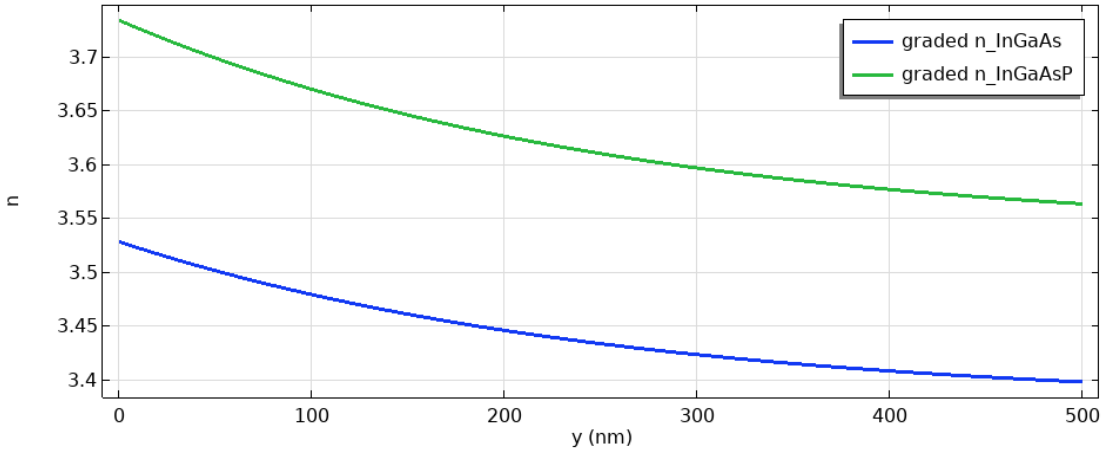

Figure 3 Graded refractive index for InGaAs and InGaAsP as a function of thickness of active layer

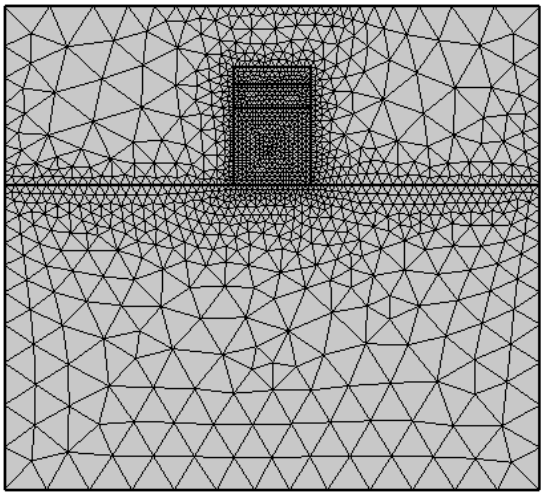

Figure 4 Mesh for the structure

Propagation length and confinement:

One property of the surface plasmon is the Lp of the SPP waveguide since it has an effective refractive index (Neff). Here, Lp depends on the imaginary part of it according to the following relationship SPP waveguide $Lp = 1/(2k_0 n''_{eff})$[26], where n''_{eff} is the imaginary part of the effective refractive index ($n_{eff} = n'_{eff} + in''_{eff}$) of the HSPP waveguide and ($k_0 = 2\pi/\lambda$) is the wavenumber in space[27] [28].

We propose a plasmonic waveguide that fulfills both deep subwavelength scale confinement and relatively long propagation. The waveguide comprises a metal cap (nano tape) on top, which confines light between the interface of the metal-insulator. Here, we developed a hybrid plasmonic waveguide architecture in which the

SPP is nanoscale confined in a waveguide. In terms of the figure of merit, this structure outperforms current plasmonic waveguides, making the waveguide particularly suitable in photonic integrated circuits. We have generated a hybrid plasmonic waveguide design in which the SPP is confined to a nanoscale waveguide. This structure outperforms existing plasmonic waveguides in terms of the figure of merit, making waveguides particularly useful in optical integrated circuits. The confinement is calculated using a certain parameter mode area and FoM. To find a definition that will consider the true extent of the SPP field distribution to consistently quantify the mode confinement. We will provide several definitions and compare them in our study of different waveguide structures. The first definition evaluates mode confinement in the modal area A_{eff} depending on the peak energy flux density and is defined as[29] [30] [9].

$$A_{eff1} = \frac{\int \boldsymbol{p}(\mathrm{x,y})\mathrm{dxdy}}{\max[\boldsymbol{p}(\mathrm{x,y})]} \qquad (6\mathrm{A})$$

$\boldsymbol{p}(\mathrm{x,y})$mean energy flux density (Poynting vector), $\boldsymbol{p}(\mathrm{x,y}) = [\boldsymbol{E}(x, y) \times \boldsymbol{H}(x, y)]$. The normalized modal area is defined as (A_{eff1}/AO) [31], where *AO* represents the diffraction-limited area in free space, $A0 = \lambda^2/4$. Here, λ is the vacuum wavelength. A_{eff} is based on maximum power flux density and can be used to estimate confined field enhancement that is not necessarily associated with a strong limitation of the total power. The second definition A_{eff2} is a statistic that represents the integral of the energy density *W* throughout the proposed design's cross-section. [32] [33]

$$A_{eff2} = \left[\int_{A\infty} W(r)dA\right]^2 \Big/ \int_{A\infty} W(r)^2 dA \qquad (6B)$$

A better scale often considers the entire field and is more sensitive to the power distribution. Another problem comes when we try to analyze the performance of a specific waveguide structure. Although most plasmonic waveguides function using the same plasmonic phenomena, they have different diffusion and confinement characteristics. Any structure's FoM form must account for all of these factors. We must use an appropriate definition of collateral to determine the FoM form because the propagation distance is well specified. [29] [34] $FoM = \frac{L_p}{\lambda_0}/\frac{A_{eff2}}{A_0}$ The ratio of Lp to the diameter of the mode field is also known as FoM:

$$FoM = \frac{L_\mathrm{p}}{2\sqrt{\frac{A_{eff}}{\pi}}} \qquad (7)$$

the normalized mode field area ($A = A_{eff}/A0$) [29].

Results and Discussions:

Table 1 The parameters of the structure

Parameters	Values

©SRP 2024, DOI: https://doi.org/10.47758/ijnsn.v5i1.120

width of ridge	0.5[µm]
main wire width	3000[nm]
Refractive index InGaAsP static (y=1)	n=3.7336
Refractive index InGaAs (x=0.4)	3.5279
Refractive index InGaAsP static (y=0)	3.5355
Refractive index InGaAs (x=0 =GaAs)	3.3767
Refractive index InGaAs (x=0.5)	3.1779
Refractive index InP	3.1669
Refractive index InGaAsP	3.3636
Refractive index _gold(real+image)	0.187+10.3457*i
Wavelength	1.55[µm]
gold thickness	110[nm]
InP thickness	160[nm]
Core thickness	0.5[µm]

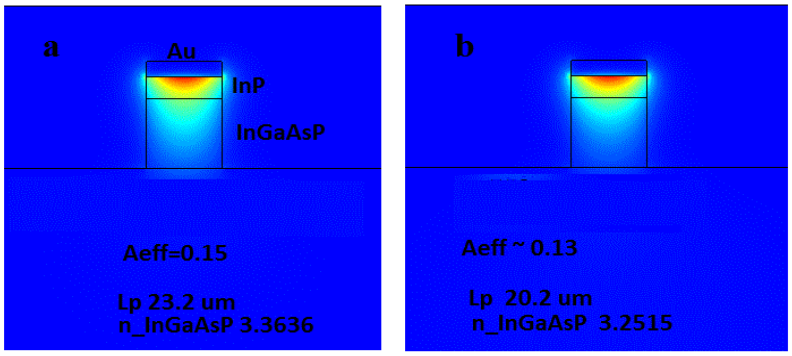

Figure 5 Electric field norm (|E|) distribution of the basic mode in an InP-based HP waveguide. w=500 nm h_InGaAsP=500 nm=h_InGaAs. The refractive index for InP and gold (Au) is 3.1669, and 0.187+10.3457i. (a) y=0.461[21] and 3.2515. (b) In cases x=0.48 and y=0.24, the refractive index for InP and gold (Au) is 3.1669 and 0.187+10.3457i.

Fig. 5 Based on a semi-insulating InP substrate, there is a 500 nm InGaAsP core layer and a 160 nm InP top cladding layer. Gold (Au) or silver (Ag) with a thickness of 110 nm caps the layer stack of the hybrid plasmonic waveguide. During the simulation of passive devices, the thickness of the capped metal is tuned to improve power transfer from input waveguides to output waveguides. At a wavelength of 1550 nm, the two refractive indices of $In_{1-x}Ga_xAs_yP_{1-y}$ (Q(1.25)) are 3.3636 (a) in the case of y=0.461[21] and 3.2515 (b) in the cases of x=0.48 and y=0.24, and the refractive indices for InP and gold (Au) are 3.1669 and 0.187+10.3457i, respectively. The plots of the first four TM modes, as well as the related mode profiles, for the HP-waveguide at a wavelength of 1.55 m appear in Fig. 6. The fundamental TM_{00} mode in the HP-waveguide has no cutoff, and the number of modes supported by the HP-waveguide grows with the width of the ridge. As the width of the ridge grows, the real part of the effective refractive index approaches that of the InGaAsP layer. The optical power is dispersed throughout the InGaAsP core layer in a deeply etched conventional waveguide, whereas it is concentrated mostly within the InP cladding layer in an HP waveguide.

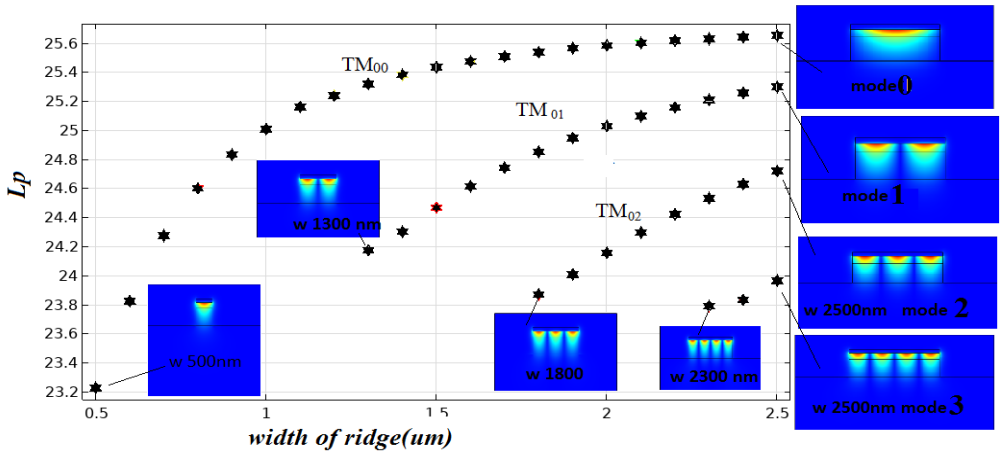

Figure 6 Lp of the structures for the InP-based HP waveguide for the TM00, TM01, TM02, TM03, and TM04 patterns, dependent on the imaginary part of the refractive indices. The norm and direction of electric field distribution TM modes for (mode0) fundamental mode (mode1) first mode (mode2) second mode and (mode3) third mode Patterns are formed when the width of the HP waveguide is increased.

The propagation length is greater than 15 μm for all ridge widths depicted in Fig. 6. The largest Lp does not exceed 26 μm for the first mode and is less than that for the rest of the three modes despite the increase in the dimension widths of the ridge from 500 nm up to 2500 nm. Comsol software was used to determine the effective refractive index and electrical field distribution of InP-based conventional and HP waveguides. By using mode analysis, Fig. 6 and Fig. 7 show the Lp for the two InGaAsP refractive indices, so Fig. 8 gives the effective mode index for the two InGaAsP refractive indices in the two TM modes TM_{00} and TM_{01}, with a refractive index of 3.3636 being longer than the refractive index of 3.2515 and a refractive index of 3.3636 being the longest but with less quantum confinement than the refractive index of 3.2515, as indicated by the parameters A_{eff}& FoM. Figures 9 & 10 present it as well.

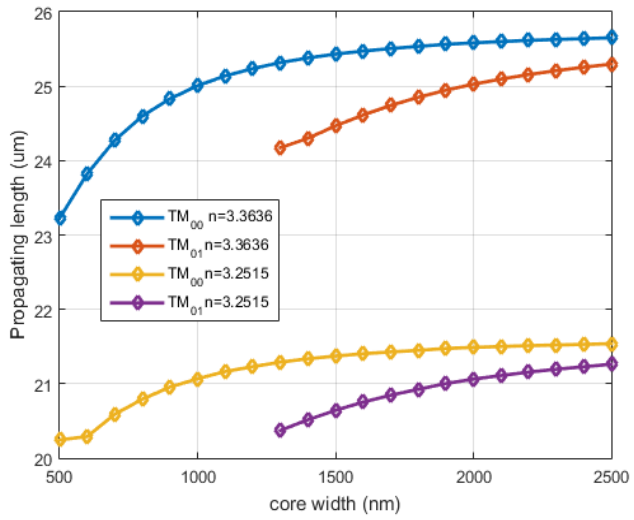

Figure 7 propagation length for the two InGaAsP refractive indices, with the refractive index of 3.3636 being longer than the refractive index of 3.2515

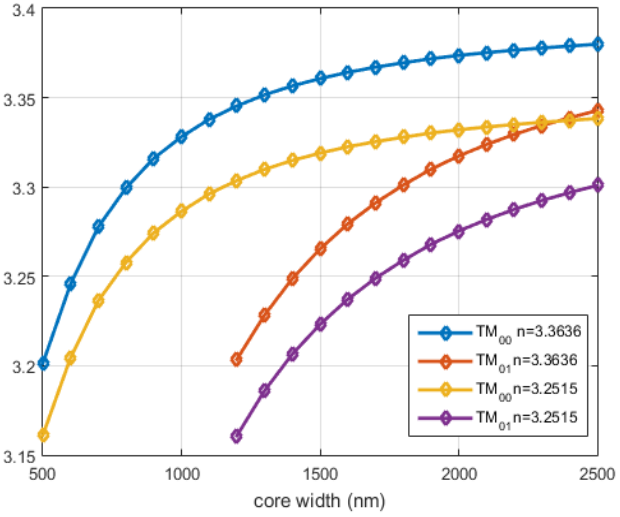

Figure 8 Effective mode index for the two InGaAsP refractive i

Figure 10 Figure of merit for n_InGaAsP 3.3636 and 3.2515 to r increase the width in x-axes

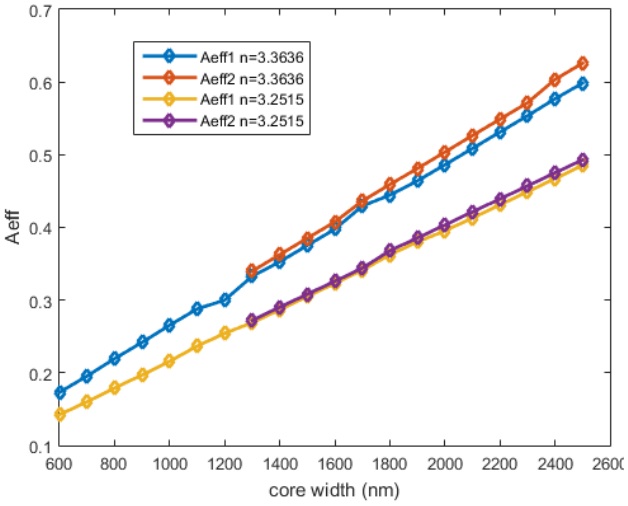

Figure 9 A_eff1 and A_eff2 for n_InGaAsP 3.3636 and 3.2515 to increase the width in x-axes, used in two equations (3 and 4)

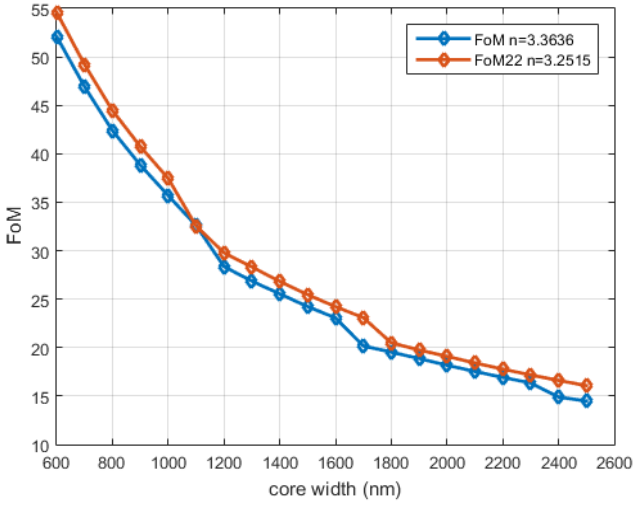

The Graded-index GRIN configuration is analyzed in the radio frequency (RF) section of COMSOL, which is the latest version of the software. A two-dimensional model is created and simulated at the telecom wavelength of 1.55 µm. The Lp of the SPP wavelength propagating along the surface of the metal and its mode width is calculated and drafted below.

Fig. 11 shows the modes versus width of ridge dimensions w=500 nm to w=2500 nm. Fig. 11 corresponds to the structure with a GRIN square ridge, and Fig. 6 corresponds to the structure with a constant-index square ridge. Introducing the graded into the refractive indices of InGaAs, InGaASP by changing the doping ratios of the mole fractions (X and Y), will be done in two ways: stabilizing the X ratio and changing the doping ratio y

mole fraction, and changing the X ratio and then conducting analysis and simulation of the resulting field using the Comsol Multiphysics program. It determines the Lp and the amount of quantitative confinement, as well as whether these parameters have improved. The Lp as well as the parameters used to measure confinement, namely, the area mode and the figure of merit, are shown in the next three figures (11, 12 and 13). By fixing X and scaling with the mole fraction 1 > Y > 0, we obtain a graded refractive index (3.5355 - 3.7336) that is better in value than the second case, which uses the tertiary material InGaAs 1 > X > 0 and gives us a refractive index ranging from 3.5279 to 3.3767, as seen in the simulations and calculations in the figures underneath. In the first structure, Lp varies between 32 µm at a 400 nm ridge width and 40.18 µm at a 2500 nm ridge width. In terms of enumeration parameters, as in Fig. 12, the mode area is better in the first case than in the second case, and Fig. 13 shows that the parameter FoM is similar in both situations. As a result, the limitation in the hybrid plasmonic waveguide is that it maintains its quality without waste.

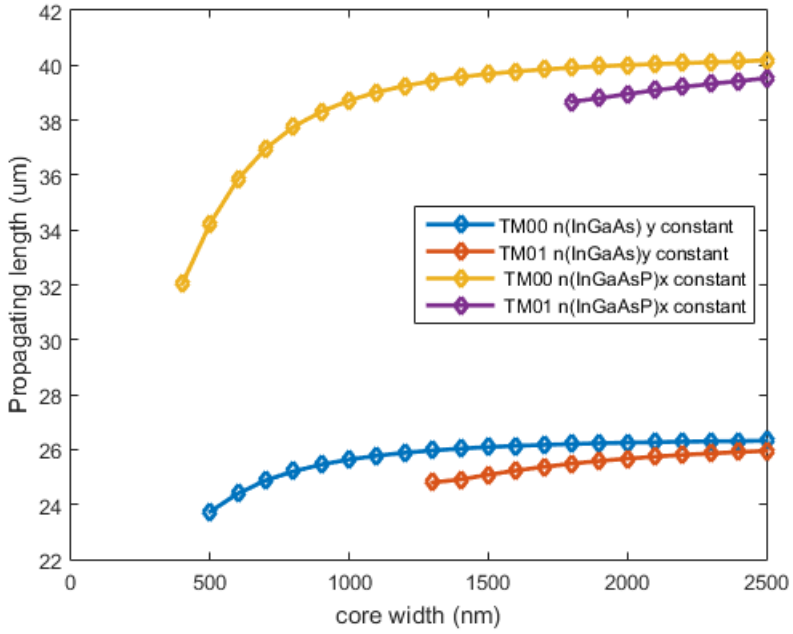

Figure 11 The Lp in the first case using the quaternary material InGaAsP was determined by fixing X and scaling with the mole fraction 1 > Y > 0, and we obtained a grade in the refractive index (3.5355 - 3.7336) that was better in values than the second case when using the tertiary material InGaAs 1 > X > 0, in which we included it in the refractive index from (3.5279- 3.3767).

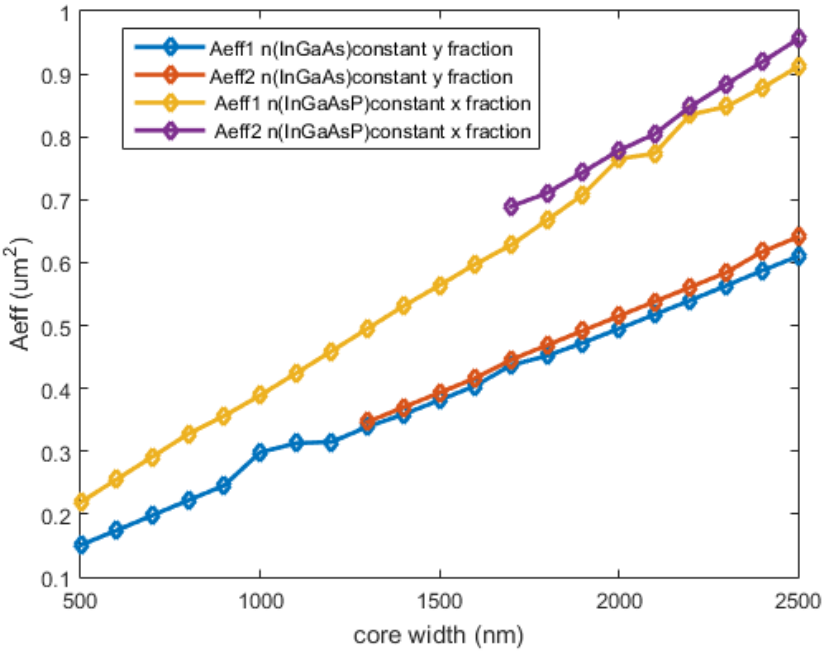

Figure 12 shows the A_{eff} mode area parameters used in two equations (3 and 4) that were used in the confinement measurement. By setting X and scaling with the mole fraction 1 > Y > 0, the first case using the quaternary material InGaAsP yielded a refractive index gradient that was better in values than the second case using the tertiary material InGaAs 1 > X > 0.

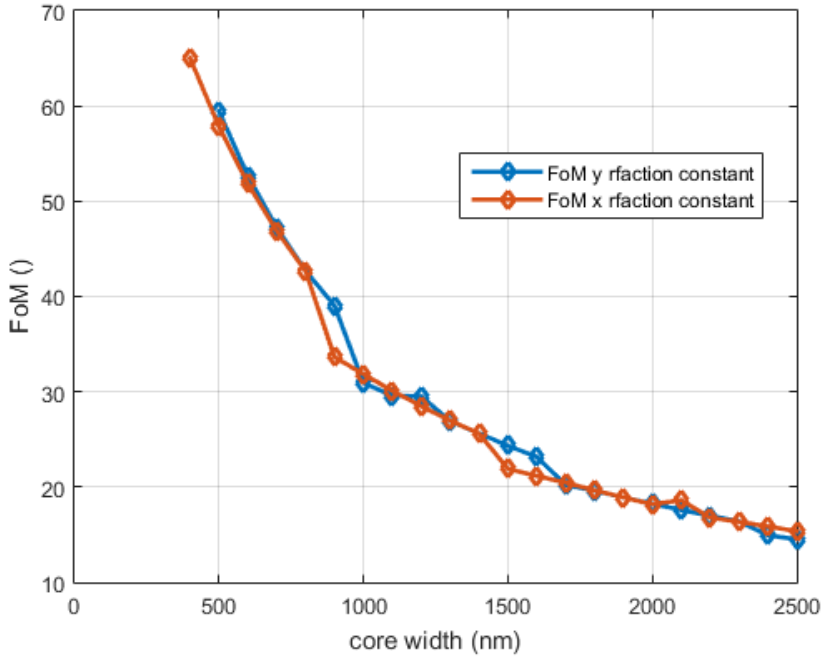

Figure 13 shows the FoM number of the merit parameter used in confinement measurement. InGaAsP Gradad in refractive index was very close in value to the second case when using the tertiary material InGaAs.

When replacing the aforementioned wavelength 1.550 µm to 0.633 µm and applying the same previous

parameters, we found that there is a jump in Lp 10 µm to reach more than 70 µm for the quaternary compound InGaAsP while retaining the quantitative confinement value in width=500 nm with indices Figures 16, 15, 14 indicate that A_{eff} = 0.1 m2, FoM = 88 is also better than the prior case: A_{eff} = 0.15 m2, FoM = 60.

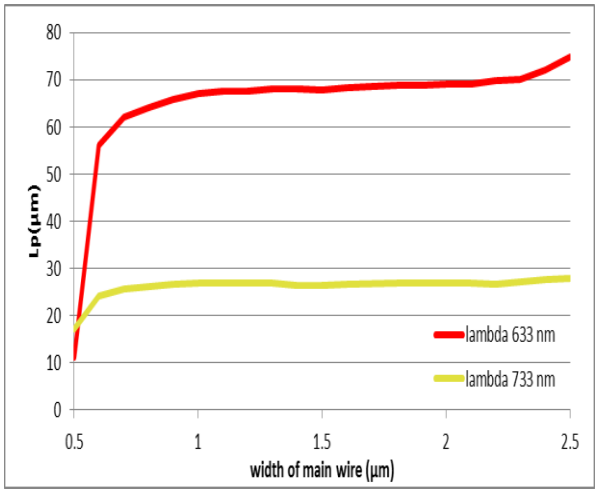

Figure 14 Lp for graded index HSPP at wavelengths 633 nm and 733 nm.

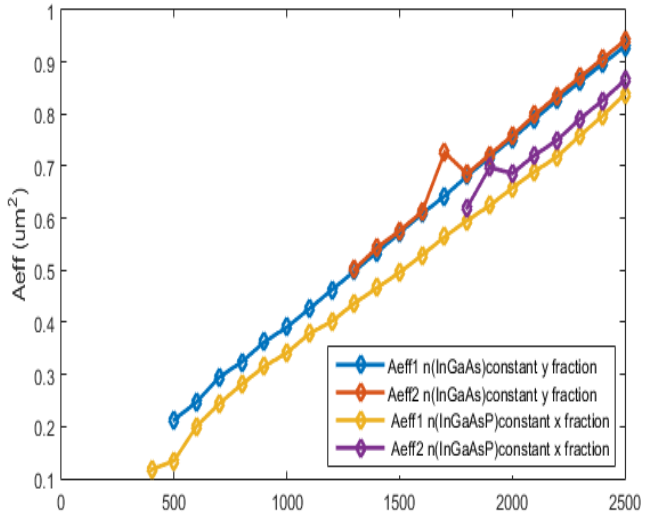

Figure 15 Aeff1 and Aeff2 for graded index HSPP at wavelengths 633 nm and 733 nm.

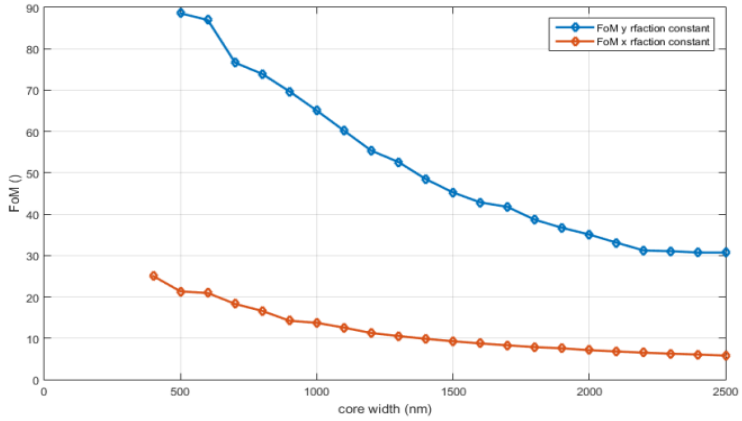

Figure 16 FoM for graded index HSPP at wavelengths 633 nm and 733 nm.

Conclusion:

A graded-index waveguide for SPP was suggested, enabling light focus and longer distance propagation. The graded-index design has been developed using the effective index method and numerically analyzed with the COMSOL Multiphysics program. In contrast to prior approaches for HP plasmonic waveguides, Lp was twice as much in case the graded refractive index for InGaAsP was greater than that for InGaAs and conservative

confinement. Because our method is scalable to telecom wavelengths, it is expected to spur more research into plasmonic multimode-interference devices based on traditional waveguide optics design techniques.

The best results were in the case of the gradient in the refractive index of the quaternary compound InGaAsP, in which the value of Lp = 40.18 µm was reached, which is twice its value in the base case.

All of the above was at a wavelength of 1550 nm, but at frequencies of 633 nm, there was a large jump in Lp to reach more than 71 nm, the confinement remains good, and the amount of FoM is greater and better clear in Figs. 14, 15 and 16.

References

[1] J. Wen *et al.*, "Numerical investigation of on-chip wavelength conversion based on InP/In1−xGaxAsyP1−y semiconductor waveguide platforms," *Opt. Commun.*, vol. 473, no. April, p. 125921, Oct. 2020, doi: 10.1016/j.optcom.2020.125921.

[2] A. Bernard *et al.*, "Mid-infrared optical characterization of InGaAsP," *J. Opt. Soc. Am. B*, vol. 35, no. 12, p. C25, 2018, doi: 10.1364/josab.35.000c25.

[3] B. Jensen and A. Torabi, "Refractive index of quaternary In1-xGaxAs yP1-y lattice matched to InP," *J. Appl. Phys.*, vol. 54, no. 6, pp. 3623–3625, 1983, doi: 10.1063/1.332402.

[4] M. P. C. Krijn, "Heterojunction band offsets and effective masses in III-V quaternary alloys," *Semicond. Sci. Technol.*, vol. 6, no. 1, pp. 27–31, 1991, doi: 10.1088/0268-1242/6/1/005.

[5] M. Smit *et al.*, "An introduction to InP-based generic integration technology," *Semicond. Sci. Technol.*, vol. 29, no. 8, p. 083001, Jun. 2014, doi: 10.1088/0268-1242/29/8/083001.

[6] X. Zhang *et al.*, "Heterogeneous 2.5D integration on through silicon interposer," *Appl. Phys. Rev.*, vol. 2, no. 2, 2015, doi: 10.1063/1.4921463.

[7] J. and D. P. Capmany, "Programmable integrated photonics," in *Emerging Applications in Silicon Photonics*, Oct. 2020, p. 344, doi: 10.1117/12.2584904.

[8] V. J. Sorger, R. F. Oulton, R. M. Ma, and X. Zhang, "Toward integrated plasmonic circuits," *MRS Bull.*, vol. 37, no. 8, pp. 728–738, 2012, doi: 10.1557/mrs.2012.170.

[9] J. Xiao *et al.*, "A CMOS-compatible hybrid plasmonic slot waveguide with enhanced field confinement," *IEEE Electron Device Lett.*, vol. 37, no. 4, pp. 456–458, 2016, doi: 10.1109/LED.2016.2531990.

[10] I. A. Pshenichnyuk, S. S. Kosolobov, and V. P. Drachev, "Toward deep integration of electronics and photonics," *Appl. Sci.*, vol. 9, no. 22, pp. 1–16, 2019, doi: 10.3390/app9224834.

[11] S. Lien and C. Ng, *physics of Op toelectronic Devices*. john wiley, 1995.

[12] J. A. A. Engelbrecht, "An assessment of some theoretical models used for the calculation of the refractive index of InXGa1−xAs," *Phys. B Condens. Matter*, vol. 535, no. May, pp. 8–12, 2018, doi: 10.1016/j.physb.2017.05.047.

[13] M. Nikoufard, M. K. Alamouti, and S. Pourgholi, "Multimode Interference Power-Splitter Using InP-Based Deeply Etched Hybrid Plasmonic Waveguide," *IEEE Trans. Nanotechnol.*, vol. 16, no. 3, pp. 477–483, 2017, doi:

10.1109/TNANO.2017.2688397.

[14] M. A. Mahdian, M. Nikoufard, and F. Soleimannezhad, “Effect of etching depth on the performance of InP-based hybrid plasmonic waveguides,” *AEU - Int. J. Electron. Commun.*, vol. 126, no. August, p. 153403, 2020, doi: 10.1016/j.aeue.2020.153403.

[15] M. Sotoodeh, A. H. Khalid, and A. A. Rezazadeh, “Empirical low-field mobility model for III-V compounds applicable in device simulation codes,” *J. Appl. Phys.*, vol. 87, no. 6, pp. 2890–2900, 2000, doi: 10.1063/1.372274.

[16] S. J. Sweeney and J. Mukherjee, “Optoelectronic devices and materials,” in *Springer Handbooks*, no. January 2017, S. Kasap and P. Capper, Eds. Boston, MA: Springer US, 2017, p. 1.

[17] C. Chan, S. L. Ng, and L. Lam, “InGaAslInGaAsP quantum well infrared photodetector array operating at 1.5J. m wavelength,” pp. 141–144, 2000.

[18] S. Adachi and C. W. Tu, “Physical Properties of III-V Semiconductor Compounds: InP, InAs, GaAs, GaP, InGaAs and lnGaAsP,” *Phys. Today*, vol. 47, no. 2, pp. 99–100, 1994, doi: 10.1063/1.2808406.

[19] S. Seifert and P. Runge, “Revised refractive index and absorption of In_1-xGa_xAs_yP_1-y lattice-matched to InP in transparent and absorption IR-region,” *Opt. Mater. Express*, vol. 6, no. 2, p. 629, 2016, doi: 10.1364/ome.6.000629.

[20] B. Optoelectronics, “Refractive index n of AlGaAs,” pp. 2–4, 1985, [Online]. Available: batop.com/information/n_AlGaAs.html.

[21] M. Nikoufard, “Integrated wavelength division multiplexing,” Technische Universiteit Eindhoven, 2008.

[22] F. Fiedler and A. Schlachetzki, “Optical parameters of InP-based waveguides,” *Solid State Electron.*, vol. 30, no. 1, pp. 73–83, 1987, doi: 10.1016/0038-1101(87)90032-3.

[23] A. Snyder and J. Love, *Optical waveguide theory.-London: Chapman & Hall*. Springer Science & Business Media, 1983.

[24] S. Irmscher, *Design, Fabrication and Analysis of InP-InGaAsP Traveling-Wave Electro-Absorption Modulators*. 2003.

[25] COMSOL Inc., “RF module user guide v5.3a,” 2017. [Online]. Available: http://localhost:8090/docserver/#!/com.COMSOL.help.rf/html_RFModuleManual.html.

[26] Y. Chowdhury, “Plasmonic Waveguides : Design and Comparative Study,” *Thesis, MS*, p. 81, 2011.

[27] R. Tamaki, Y. Shoji, L. Lombez, J.-F. Guillemoles, and Y. Okada, “Quasi-Fermi level splitting in InAs quantum-dot solar cells from photoluminescence measurements,” *Opt. Express*, vol. 16, no. March 2020, p. 32, Jan. 2020, doi: 10.1117/12.2545657.

[28] C. Y. Chunwei Ye, Y. L. Yumin Liu, J. W. Jie Wang, H. L. Hongbo Lv, and Z. Y. Zhongyuan Yu, “Graded-index ridge surface plasmon polaritons waveguide,” *Chinese Opt. Lett.*, vol. 12, no. 9, pp. 092402–092405, 2014, doi: 10.3788/col201412.092402.

[29] T. Ma *et al.*, “Graphene-Coated Two-Layer Dielectric Loaded Surface Plasmon Polariton Rib Waveguide with Ultra-Long Propagation Length and Ultra-High Electro-Optic Wavelength Tuning,” *IEEE Access*, vol. 8, pp. 103433–103442, 2020, doi: 10.1109/ACCESS.2020.2999395.

[30] J. Wang, Y. X. Guo, B. H. Huang, S. P. Gao, and Y. S. Xia, “A Silicon-Based Hybrid Plasmonic Waveguide for Nano-Scale Optical Confinement and Long Range Propagation,” *IEEE Trans. Nanotechnol.*, vol. 18, pp. 437–444, 2019,

doi: 10.1109/TNANO.2019.2911333.

[31] Z. Zhang and J. Wang, "Long-range hybrid wedge plasmonic waveguide," *Sci. Rep.*, vol. 4, pp. 1–9, 2014, doi: 10.1038/srep06870.

[32] Y. CHOWDHURY, "plasmonic waveguide design and Comparative Study," 2011.

[33] Y. Bian *et al.*, "Highly confined hybrid plasmonic modes guided by nanowire-embedded-metal grooves for low-loss propagation at 1550 nm," *IEEE J. Sel. Top. Quantum Electron.*, vol. 19, no. 3, 2013, doi: 10.1109/JSTQE.2012.2212002.

[34] N. T. Huong, N. D. Vy, M. T. Trinh, and C. M. Hoang, "Tuning SPP propagation length of hybrid plasmonic waveguide by manipulating evanescent field," *Opt. Commun.*, vol. 462, no. December 2019, p. 125335, 2020, doi: 10.1016/j.optcom.2020.125335.